Lab on a Chip

Accepted Manuscript

ROYAL SOCIETY OF CHEMISTRY

www.rsc.org/loc

Lab on a Chip

RSCPublishing

ARTICLE

Table of entry

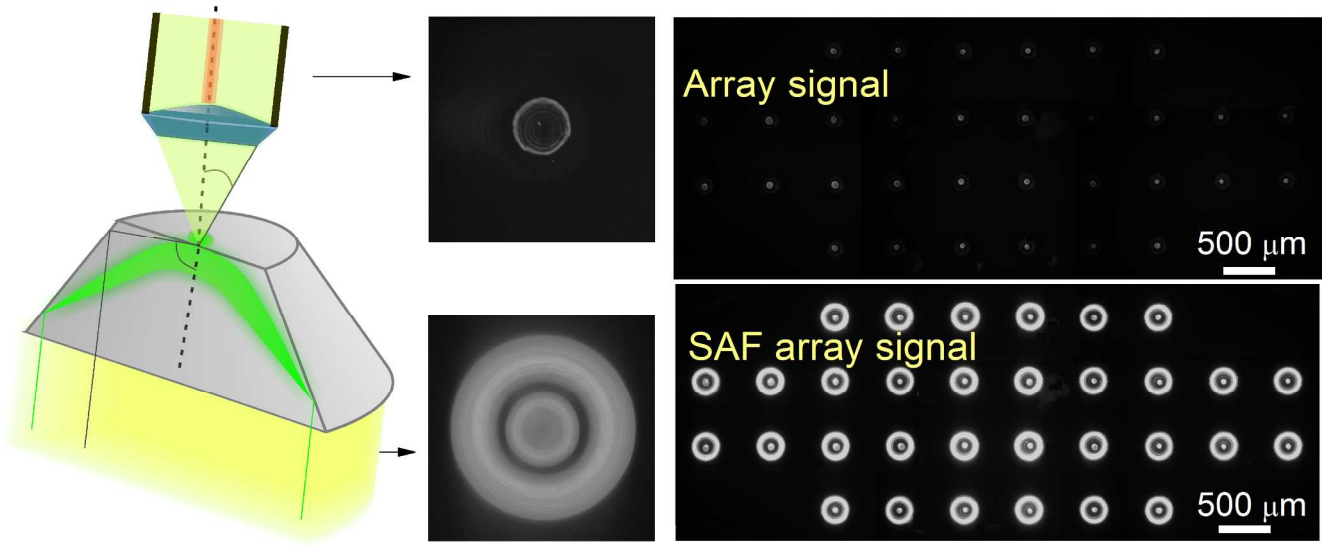

We developed a lab-on-a-chip system integrating miniaturized micro-optics SAF arrays within microfluidic chambers for highly sensitivity and multiplexed detection of fluorescent molecules

Lab on a Chip

RSCPublishing

ARTICLE

Miniaturization of a micro-optics array for highly sensitive and parallel detection on injection moulded lab-on-a-chip

Cite this: DOI: 10.1039/x0xx00000x

Received 00th February 2015,
Accepted 00th February 2015

DOI: 10.1039/x0xx00000x

www.rsc.org/

Tran Quang Hung[a,b], Yi Sun[a], Carl Esben Poulsen[a], Than Linh-Quyen[b], Wai Hoe Chin[b], Dang Duong Bang[b] and Anders Wolff[a,*]

A miniaturised array of supercritical angle fluorescent (SAF) micro-optics embedded in a microfluidic chamber was fabricated by injection moulding. The fabricated chip could enhance the fluorescent signal around 46 times compared to a conventional microscope. Collection of fluorescent signal from the SAF array is almost independent of numerical aperture, and the limit of detection was improved 36 folds using a simple and inexpensive optical detection system.

Introduction

Although many advanced technologies such as Raman spectroscopy[1] and magnetic based platform[2] have been developed for highly sensitive detection of biomolecules, fluorescence–based sensing technology is still the most widely used technique and has been so for several decades[3]. Many researches are therefore devoted to improve the sensitivity of fluorescent detection, by e.g. using a thin layer of metallic nanoparticles on a microscope slide to enhance the light-plasmon coupling[4–6] or super-resolved fluorescence microscope, which transcend the Abbe's diffraction limit of a half of the utilized wavelength ($\lambda/2$)[7–11]. Even though such methods can achieve unprecedented resolution and have detection limit down to single photon, they require very expensive optical equipment, and have very limited field of view. Such methods are therefore normally limited to central research laboratories.

Alternatively, another highly sensitive detection method based on supercritical angle fluorescence (SAF) microscopy was described by J. Enderlein *et. al*[12]. SAF is based on the principle that

fluorescent molecules near the interface of two media with different refractive index radiate highly asymmetrically. The majority of the light emits into the higher refractive index medium, mainly around the supercritical angle (θ_c). This main portion of the fluorescence light is lost in conventional system, but in a so-called SAF microscopy[13–19], where parabolic lens system has been developed as a microscope objective to collimate the light emitted into the higher refractive medium. C.M. Winterflood *et. al*., reported that by collecting the fluorescence signals above and below θ_c, the SAF microscopy system became extremely sensitive to the z – positions[20]. It was possible to discriminate surface-bound targets (within 100 nm from the surface) from the targets in the sample solution. This eliminates fluorescence "noise" from the liquid and enables for real-time study of binding kinetics at the interface. However, a conventional SAF setup measures only one detection point, which limits its application in array-based sensing. To overcome this limitation, D. Hill *et al.*, introduced a polymer biochip with an array of integrated 3 × 3 parabolic SAF structures with 3 mm diameter and a pitch of 4.5 mm[21]. This chip coupled the advantages of SAF microscopy (excellent sensitivity and good discrimination between molecule on surface and in bulk solution) with the multiplex detection capability of micro-array technology. Nevertheless, such a big size array has several disadvantages such as having limited number of detection points and requiring a large volume of sample. Miniaturization of SAF structures will provide more dense arrays to increase the multiplex detection capability. However, fabrication of high-quality micro-lens with parabolic shape is extraordinary difficult and requires sophisticated know-how and clean-room fabrication expertises[22]. To our knowledge there has been no report on minimization of SAF microarray and this is still a big technological challenge. Here, we addressed this challenge by introducing a truncated cone-shaped SAF structure. The cone shape can collect light at large collection angle, and it can easily be fabricated by combining micro-milling and injection moulding techniques.

In this paper, we advance our research on SAF micro-array[23] by fabricating a disposable chip with a miniaturised SAF array integrated in a microfluidic chamber for collection of fluorescent signal. The work involves the calculation of proportional of the light emitted into different polymers substrates and simple fabrication techniques for minimization of the SAF microarray with low surface roughness. Furthermore, we constructed a low cost optical read-out setup using off-the-shelf components to measure the signal from SAF array. Finally the low detection limit of the system was demonstrated.

The platform provides a much more sensitive and specific biophysical tool for applications that demand parallel analysis of molecular interactions in sub-nanolitre volumes. It can be widely used in molecular biological and genomic research for *e.g.* gene expression and point mutation/single-nucleotide polymorphism (SNP) analysis.

Materials and methods

Injection moulding of the chips

The injection moulding insert was milled in hard aluminium (alloy 2017, MetalCentret, Denmark) using a computer controlled micro-milling system (Folken Ind., Glendale, California, USA) followed by polishing (metal polish, autosol, USA). Arrays of 32 truncated cone-shape holes were milled using a 60^{o} milling tip DIXI 7006 (DIXI, Le Locle, Switzerland) as master for injection moulding of the SAF arrays.

The chips had the dimension of a microscope slide (76 mm × 25 mm × 1 mm) and were moulded in-house in polystyrene (PS) 158 K (BASF SE, Germany) using an Victory 80/45 Tech injection moulding system (Engel, PA, USA). The chip has eight chambers located parallel at the centre of the chip with a pitch of 9 mm. Each chamber had a volume of 10 μL and contained a miniaturized SAF array of 32 truncated cone-shape structures. The dimensions of the polymer chip, the

microfluidic chamber and the SAF structure are illustrated in Fig. 1. Microfluidic channels with width of 0.35 mm and depth of 0.4 mm led from the chambers and connected these to 0.8 mm diameter inlet and outlet through holes suitable for connection with a multichannel pipetting system. A 254 µm-thick film of Cyclic olefin copolymer (COC) was bonded on the chip using an ultrasonic welder (USP 4700, Techsonic, Herstad+Piber, Denmark) and trigger force of 750 N, energy 70 W·s, and hold time 0.35 s.

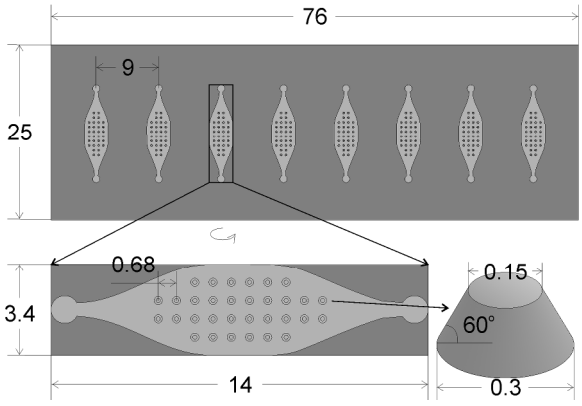

Fig. 1 Schematics illustrating dimensions of a polymer chip, a microfluidic chamber and a SAF structure (all dimensions are in mm). The pitch between the SAF structures is 0.68 mm to avoid interference of fluorescent light from nearby SAF structures.

Measurement of the surface roughness

Surface roughness of the SAF structures will give light scattering effects, especially at the sidewall of the SAF structures where the fluorescent light is collected using total internal reflection (TIR, see results Fig. 4e and 4f). To characterize the roughness of the sidewall surface we engineered a holder with a slope angle of 60 degrees and then mounted a piece of the injection moulded SAF structure on this surface to level the sidewall relatively to the instrument. The roughness of the SAF structures was characterized using a PLu Neox 3D optical profiler (Sensorfar, USA) with a vertical resolution less than 2 nm.

Detection system

We developed a simple and inexpensive optical setup for detection of Cy3 fluorescent signal from the SAF array as illustrated in Fig. 2. The optical setup comprised of off-the-shelf components: A green solid state laser (532 nm, 200 mW) (DX, Hongkong, China) was expanded 4 times using a beam expander with two achromatic lenses: f_1 = 19 mm, Ø = 0.5", f_2 = 75 mm, Ø = 1" (Thorlabs, New Jersey, USA). The central part of the expanded beam, which had an intensity variation of less than 0.3 %, was used to illuminate the entire SAF array. The filter cube for Cy3 fluorescence included a 45° green dichroic mirror 532nm±8nm/650nm±8nm reflection/transmission band, and band-pass filters of 532±10 nm (KunmingYulong, China) and 620±26 nm (Thorlabs, New Jersey, USA) for excitation and emission, respectively. The emission light from SAF array was recorded using a Prosilica camera (EC1380, Allied Vision, USA) with numerical aperture (NA) of 0.12.

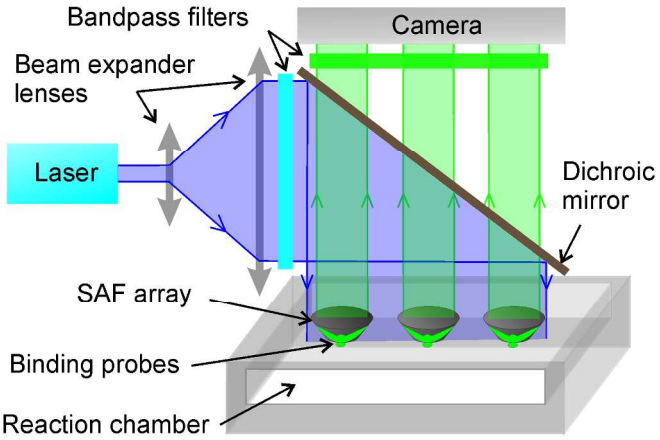

Fig. 2. Working principle of the optical setup to measure fluorescent signal from SAF array.

Deposition and immobilization of the probes

A DNA oligonucleotide probe with a poly(T)10-poly(C)10 binding sequence was used for testing the system. The binding sequence enabled direct immobilization of the probe to the plastic substrates by using a simple UV cross-linking technique described previously[24]. The probe was

labelled with Cy3 at the 5' end for visualization. The probe was diluted in 150 mM sodium phosphate buffer (pH = 8.5) containing 0.004% Triton X to final concentrations from 3.15 pM to 31.5 μM. Spotting was performed using a noncontact array nano-plotter 2.1 (GeSim, Dresden, Germany) fitted with a Picoliter pin (Pico-Tip J, GeSim, Dresden, Germany). 100 pL drops of DNA probe was spotted onto the top of each SAF structure, resulting in a spot size of approximately 70 μm. The chips were incubated at 37 ^{o}C for 10 min and then exposed to UV irradiation at 254 nm with an energy density of 0.3 J/cm^2 using Stratalinker 2400 (Stragtagene, CA, USA). Hereafter, the chips were washed in 0.1× standard saline sodium citrate (SSC) with 0.1% (w/v) sodium dodecyl sulphate (SDS) (Promega, WI, USA) solution, and rinsed in deionized water followed by drying using nitrogen gas.

Results and discussion

Selection of polymers and design SAF structure

In many applications, the fluorophores in a DNA array are detected on a dry substrate. However, for real-time analysis in a microfluidic system the DNA array will be covered with buffer solution. To select a suitable substrate for fabrication of the disposable chips, we calculated the proportion of the light emitting into the chip part as a function of its refractive index for two interfaces: air/substrate and water/substrate. In the calculation, we considered that the fluorescent molecule (dipole) emits into the lower refractive index environment n_1 by two terms, reflection and scattering, whereas the light emitted into higher refractive environment n_2 only consists of a transmission term. The intensity of the light emitting into the substrate as a function of refractive index was calculated analytically and given in Fig. 3 [see S1 for details].

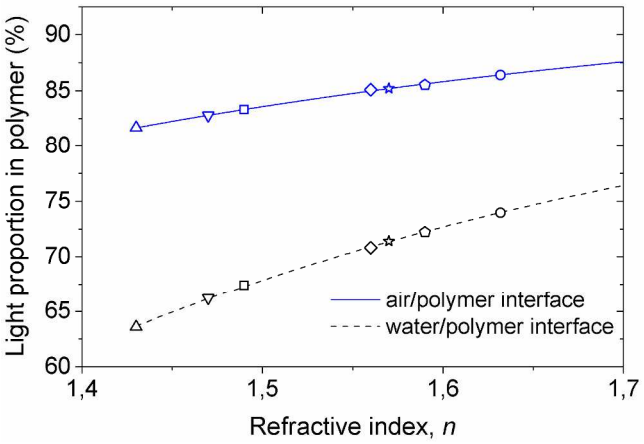

Fig. 3 The proportion of the fluorescent intensity emitting from a fluorophore sitting on the interface into the polymers (chip part) as a function of their refractive indexes of air/polymers (blue curve) and water/polymers (black curve), respectively. The symbols represent glass and polymers with different refractive indexes: △ PDMS (n = 1.43); ▽ Pyrex glass (n = 1.47); □ PMMA and PP (n= 1.49); ◇ COC (n = 1.56);☆ PET and PC (n = 1.58);⬠ PS (n = 1.59); and ○ PE (n = 1.63).

The results in Fig. 3 reveal that the fluorophores on the interface of air/substrate emits higher portion of the fluorescent intensity into the substrate than the water/substrate interface. Moreover, the higher the refractive index of the substrate, the more of the fluorescent light emits into it. As seen in Fig. 3, PS has a high light collection proportion and, furthermore, it is the most commonly used thermoplastic for laboratory culture ware and utensils[25]. Additionally, good transparency and low cost makes PS an excellent polymer for replication of the SAF structures.

To design the chip, we calculated the distribution of the fluorescent intensity emitting into the PS substrate for fluorophores on air/PS and water/PS interfaces. The polar plot and 3D graph of the fluorescent intensity distribution in the two mediums are calculated from equation 1 and 2 in S1 and given in Fig. 4. The calculations reveals that the fluorescence radiated into the PS substrate amounts to 85.56 % and 72.1 % of the total intensity for air/PS and water/PS interfaces, respectively. A parabolic lens is the best structure to collimate these proportions of fluorescent

light. However, it is very difficult to fabricate such a structure at small scale. In this work, we introduce a truncated cone-shape SAF structure with high collection efficiency, which is shown schematically in Fig. 4e. Theoretically, this truncated SAF structure can collect the light emission angle up to 79.2° and 63.2° for air/PS and water/PS interfaces, respectively (maximum angle for total internal reflection). The fluorescent intensities collected by these new truncated cone SAF structures are calculated to be about 98 % (air/PS) and 78 % (water/PS) of the total fluorescent intensity collected by a perfect parabolic lens. These are excellent collection efficiencies; the truncated SAF structure is therefore suitable for detection of fluorophores on both air/PS and water/PS interfaces.

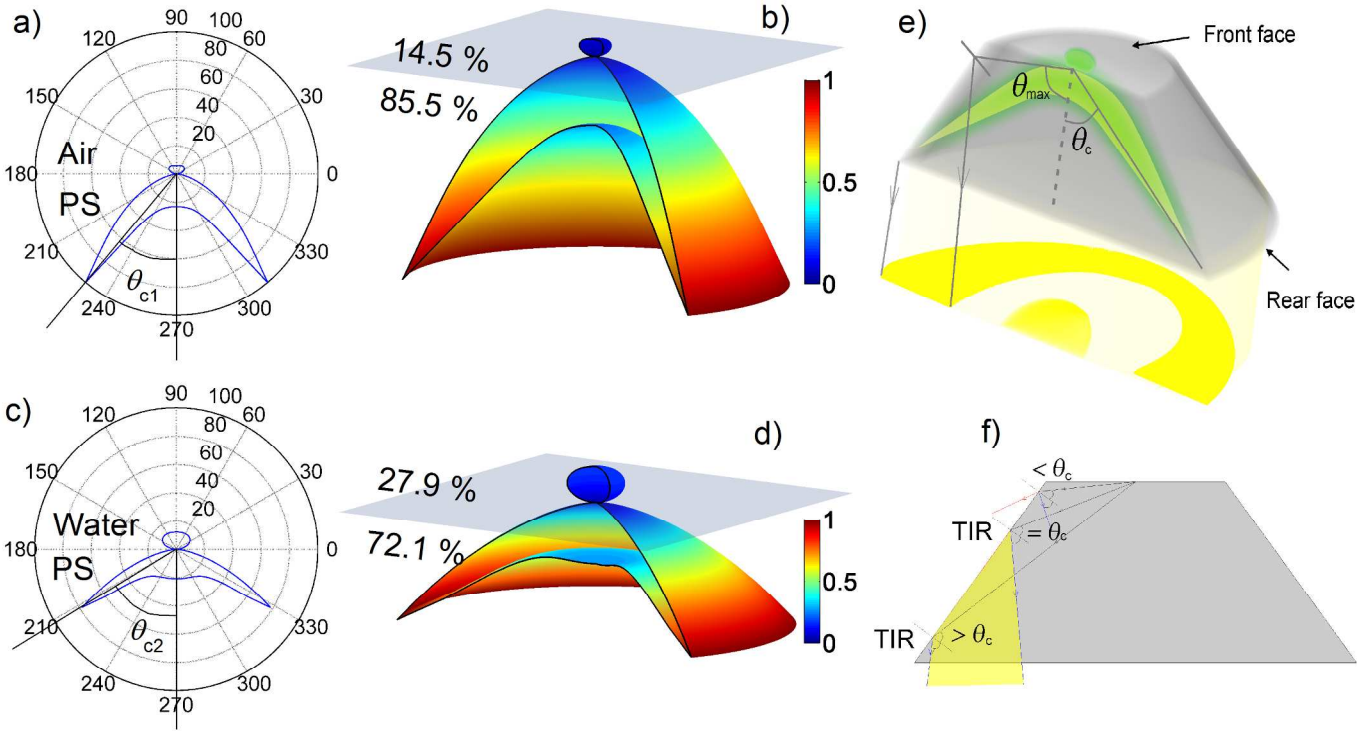

Fig. 4 (a-b) and (c-d) Theoretical calculations shown as polar plots and 3D surfaces (using equation 1 and 2 in S1) of the light intensity of fluorescent molecules distributed on air/PS and on water/PS interfaces. e) Schematic of truncated-cone SAF structure for high efficiency collection of fluorescent signal. f) Schematic of fluorescent light collection at the sidewall of a SAF structure. At $\theta \geq \theta_c$ there is total

internal reflection at the sidewall, and the fluorescent light is collected by the SAF structure. At $\theta < \theta_c$ the light is transmitted and only a small part of it is reflected and collected by the SAF structure.

Characterization of the polymer chips

SEM images of the miniaturized SAF array of 32 structures on the aluminium mould are illustrated in Fig. 5a and 5b. An image of an injection moulded PS chip with 8 chambers with SAF arrays is given in Fig. 5c.

The surface roughness of the SAF structures given in Fig. 5d was measured using an optical profilometer. The sidewall images were analysed by two parameters using Gaussian filter function: one describing the curvature and another describing the roughness of the structure [See details in S2]. The vertical resolution of these measurements is smaller than 2 nm. The average roughness of the two PS SAF array replicated from a polished and an unpolished inserts were determined to be 68 nm ± 4.8 nm and 92 nm ±15 nm respectively. Consequently, the polishing reduces the roughness of SAF structure by about 25 % from the unpolished structures. The roughness of the polished structures reaches brilliant optical quality range (~ $\lambda/8$) with small variance of about 7 %.

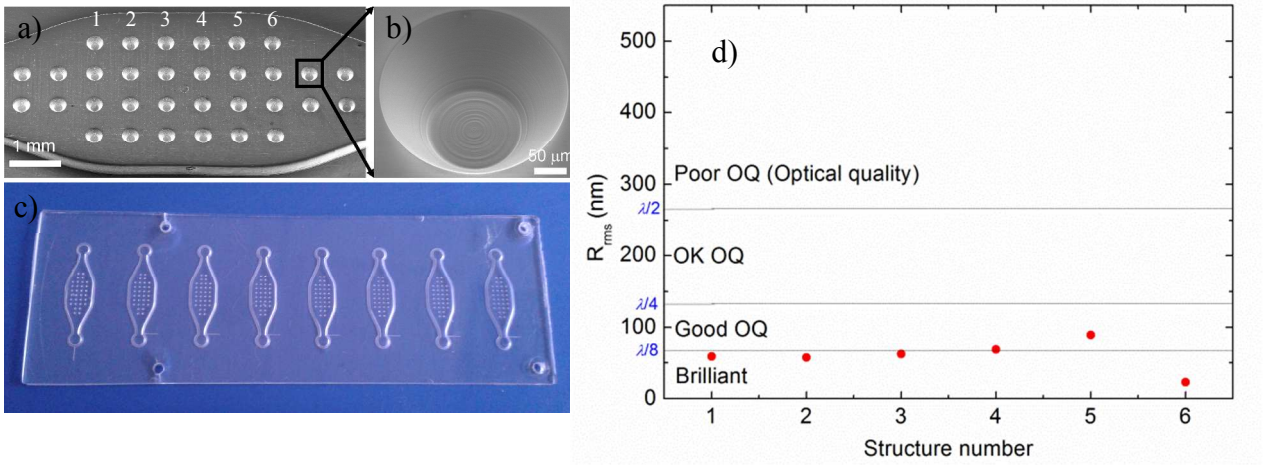

Fig. 5 a) SEM image of an array of 32 SAF structures inside a 10 μL chamber on the mould insert. b) SEM image of one structure. c) Image of a PS chip. d) Roughness of different SAF structures (same number as indicated in Fig. 5a).

Signal amplification by the SAF structures

Fig. 6a depicts fluorescent images of a micro-array captured from the front face and rear face of the SAF array using a microscope with a 5× objective and numerical aperture of 0.12. The intensity cross section of a fluorescent spot measured from both the rear and front faces of a SAF structure are plotted in Fig. 6b as solid and dot lines, respectively. The intensities are determined as grey values of the fluorescent signal from fluorescent images using ImageJ software[26]. Evident from Fig. 6b, the intensity measured from the rear face (where the SAF structure is used) is much greater than that measured from the front face (corresponding to conventional systems).

For quantification, the integrated fluorescence intensity emitted from the rear face is plotted versus the intensity from the front face of the whole SAF array as depicted in Fig. 6c. There is a linear relationship which reveals that the SAF array increases the fluorescent signal around 46 folds.

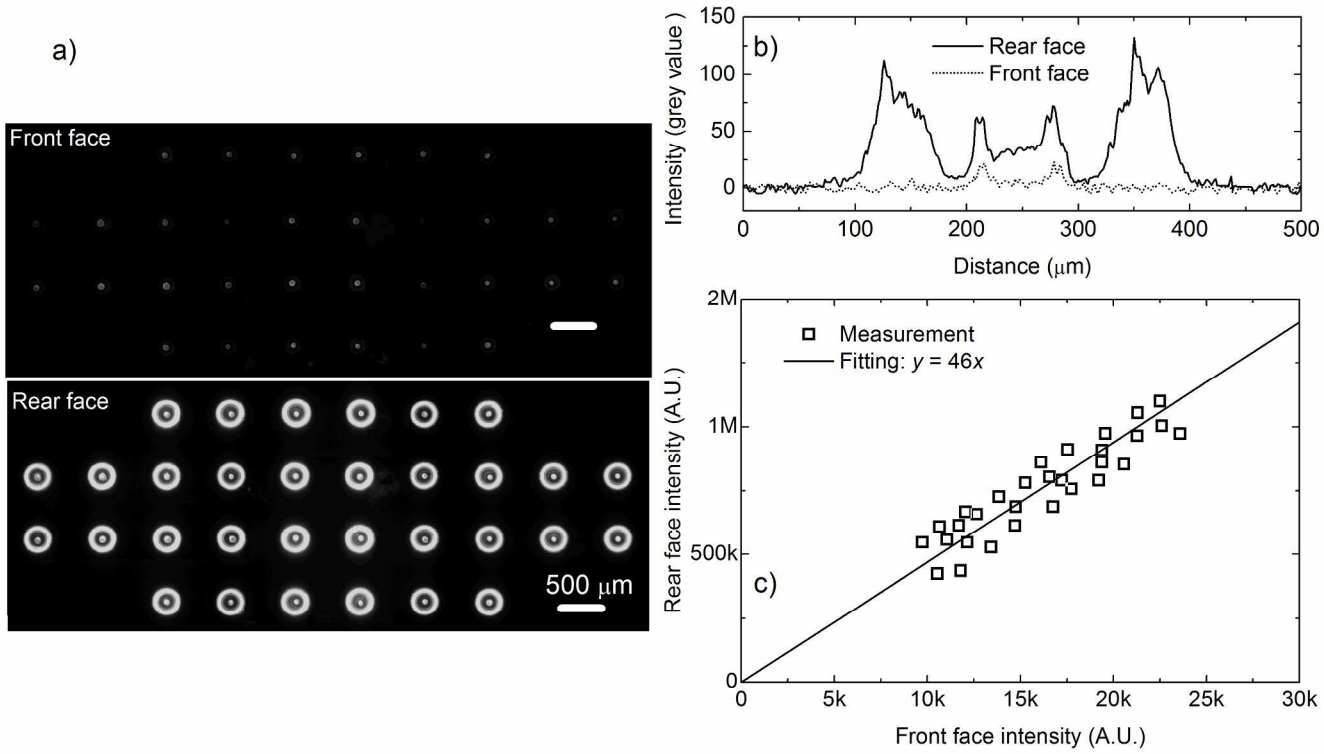

Fig. 6 a) Montage of fluorescent images of the spot array captured from the front face of the SAF structure (top image) and from the rear face of the SAF structure (bottom image). b) The fluorescent intensity plotted as greyscale across one spot measured from the front face (dotted line) and from the rear face (solid line). c) Plot of the fluorescent intensity measured from the rear face of the SAF array versus the integrated fluorescent intensity measured from the front face of the SAF array.

This high signal amplification achieved using SAF structure is ascribed to two factors:

(*i*) A greater portion of the fluorescent signal is emitted into the PS substrate than that in air. As indicated in Fig. 4b, the fluorescent intensity in PS is about 5.9 times higher than that in air.

(*ii*) The collection efficiencies in the two environments are different: In the low refractive medium (air, n_1), the collection efficiency is proportional to the numerical aperture (NA) of the optical system ~ NA×sin(θ_1) (where θ_1 is the collection angle of the objective), due to the approximately even distribution of the emission in all direction. In the high refractive medium (PS substrate, n_2), the SAF structures collect the fluorescent light within the angle range from 40.8° to

79.2^{o} due to the total internal reflection at the sidewalls of the SAF structures (Fig. 4e). Our calculations show that about 98 % of the total fluorescent light emitting into the PS substrate were collected using the SAF structures, and the light collection efficiency are therefore largely independent of the NA of the objective of the optical system (Fig. 7a).

Thus the signal ratio between the fluorescent signals from the rear face and front face of the SAF structures is a function of the NA as depicted in Fig. 7b; the measured data and the calculation are plotted as circles and solid line, respectively. In this figure, the data were collected using microscope objectives of 5×, 0.12, 4.4 mm; 10×, 0.3, 2.2 mm; 20×, 0.46, 1.1 mm; 50×, 0.5, 0.44 mm; 100×, 0.8, 0.22 mm (times magnification, NA and diameter of the field of view, respectively). In the calculation, we considered ratios between the signal collected by the SAF structures within the angle θ_{max} = 79.2^{o} in the PS substrate and the signal collected in the air medium with NA from 0.12 to 1 corresponding to the angle θ_1 varying from 6.9^{o} to 90^{o}. The calculated signal ratios are higher than the measured ones, which may be ascribed to some light scattering from the sidewall of the SAF structures (due to surface roughness) [see S3 for details] and a little transmission loss in the PS. As shown in Fig. 7b a higher NA objective leads to a lower signal ratio because the collection efficiency on the front face of the SAF structure is increased with the NA of the optical system. But a higher NA objective either has a smaller field of view as indicated in the square brackets under measurement data in Fig. 7b or requires a larger lens. In these scenarios, the SAF structures reveal prominent advantages of having both high sensitivity and a large field of view, which are desirable for high sensitive detection of multiple targets in a large area.

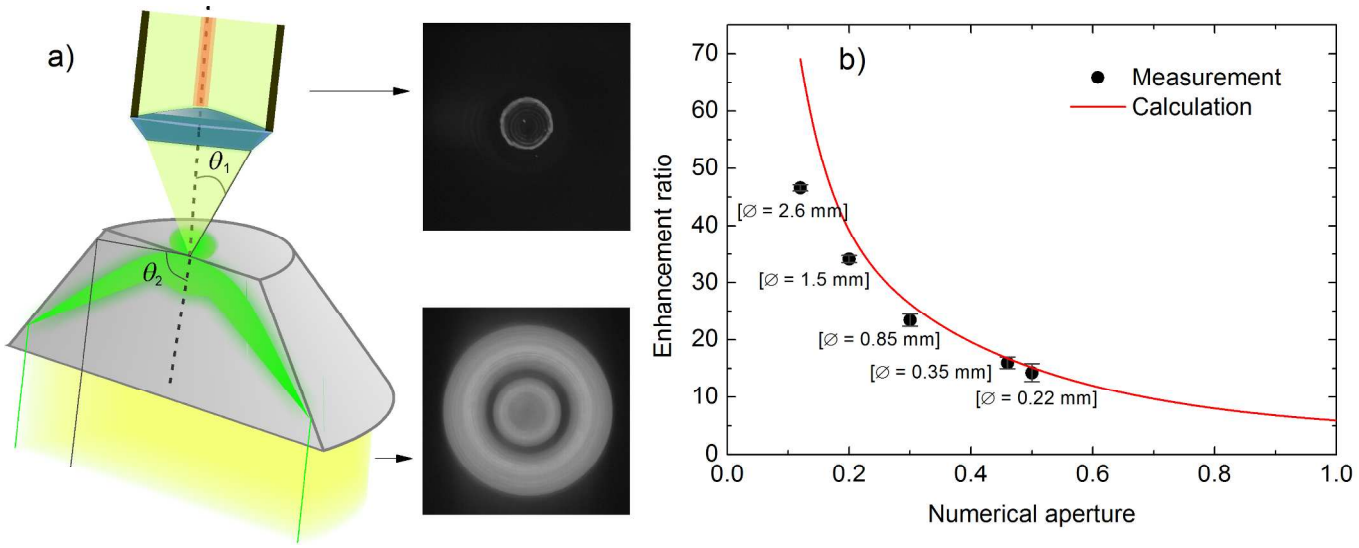

Fig. 7 a) Schematic of signal collection from the front and rear faces of a SAF structure; the two pictures on the right depict the fluorescent images from the two faces. The light collected from front face is emitted in all directions making the collection efficiency highly dependent on the numerical aperture of the optical device. In contrast, a large portion of the light from the rear face is collected by the SAF structure due to large collection angle. b) The signal amplification by SAF structure *vs*. numerical aperture of the microscope objectives. Solid line is the calculation and circles are measurement points. The numbers under measurement data represent diameters of the field of view of the optical system.

Limit of detection of the integrated LOC system

To determine the detection limit of the SAF array using a simple and low cost optical system, the Cy3 labelled DNA probe was measured on the SAF array using a 10-fold dilution series with concentrations ranging from 3.15 pM to 31.5 μM. The signal at each concentration was measured from the whole array with a 0.1 nL droplet on each SAF structure (Fig. 8a). The limit of detection (LOD) of the SAF array was calculated using the equation LOD = 3.3×SD/Slope, SD being the standard deviation of the background signal, and the slope obtained from linear fitting of the data points. The LOD of SAF array was determined to be as low as 0.5 nM corresponding to 13 fluorescence molecules per μm^2. The LOD of the signal measured from the front (air) face of the

SAF structures using the same optical system is determined as 18 nM corresponding to 468 fluorescence molecules per μm^2 as illustrated in Fig. 8b. Thus the use of SAF structures enhances the detection limit of the system by 36 folds. This factor is smaller than the signal increasing by the SAF array as discussed in Fig. 6 due to scattering from the sidewall surface of the SAF structure contributing to the background signal.

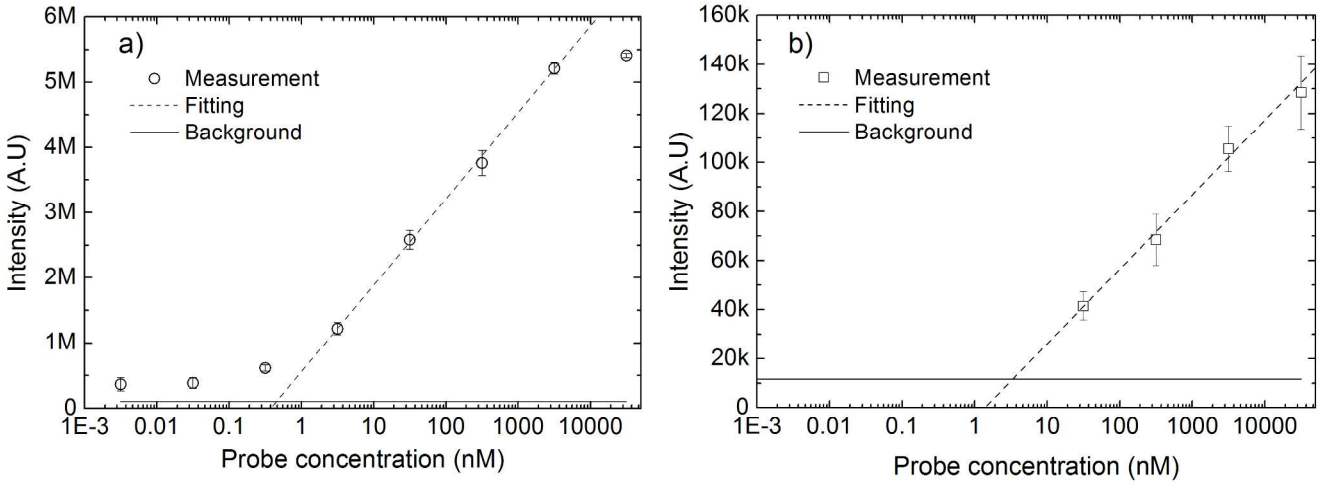

Fig. 8 The intensity of the signal *vs*. probe concentration measured from the rear (PS) face (using the SAF structures) a) and measured from the front (air) face b), using a simple optical setup. These curves correspond to the signal measured by SAF array and conventional micro-array, respectively.

Conclusions

In this paper we have presented a novel disposable chip with miniaturised SAF array integrated into a microfluidic chamber for highly sensitive detection of fluorescent molecules. The micro-optical SAF structures were realized by combining micro-milling of mould insert and injection moulding. The light intensity distributed in the two media has been calculated for different refractive indices, and based on these data PS was selected as a suitable material for replicating the SAF array. The presented SAF array reveals great advantages for multiplexed detection. It offers high sensitivity in combination with large field of view, since light collection efficiency is

largely independent from the numerical aperture of the optical system. It also provides high array density, which increases the multiplexing capability for detection of biological targets. Moreover, the detection sensitivity is very high. Fluorophore concentrations as low as 13 molecules per μm^2 could be detected using a cost effective optical readout system. In further development, a lower detection limit could be achieved by reducing the background signal and by using a higher wavelength fluorophores such as Cy5, which could minimize the scattering effect due to the roughness of the SAF structures [as calculated in S3]. Experiments of such improvements are in progressing.

Acknowledgements

This work was financially supported by the Danish Innovationsfonden - the SMARTDETECT project grand No. 118-2012-3 and Forskningsrådet Teknologi og Produktion (FTP), Sagsnr. 09066487.

Competing Interests Statement

The authors declare no competing financial interests.

Authors' Contributions Statement

Anders Wolff, Tran Quang Hung and Dang Duong Bang designed the research plan. Tran Quang Hung Yi Sun, Wai Hoe Chin, and Than Linh-Quyen performed experiments; Carl Esben Poulsen and Tran Quang Hung performed calculations. The paper has been written by Tran and has been revised by all the co-authors.

Notes and references

[a] DTU Nanotech, Department of Micro- and Nanotechnology, Technical University of Denmark, Ørsteds Plads, DK-2800 Kgs. Lyngby, Denmark.

[b] Laboratory of Applied Micro and Nanotechnology (LAMINATE) National Food Institute, Technical University of Denmark (DTU-Food), Denmark.

Electronic Supplementary Information (ESI) available: [details of any supplementary information available should be included here]. See DOI: 10.1039/b000000x/

* To whom correspondence should be addressed. E-mail: anders.wolff@nanotech.dtu.dk; Tel.: +45 45 25 63 05; Fax: +45 45 88 77 62.

1 J. Chan, S. Fore, S. Wachsmann-Hogiu and T. Huser, *Laser Photonics Rev.*, 2008, **2**, 325–349.

2 A. Sandhu, *Nat. Nanotechnol.*, 2007, **2**, 746–748.

3 S. M. Borisov and O. S. Wolfbeis, *Chem. Rev.*, 2008, **108**, 423–461.

4 M. Moskovits, *Rev. Mod. Phys.*, 1985, **57**, 783–826.

5 E. Fort and S. Grésillon, *J. Phys. D. Appl. Phys.*, 2008, **41**, 013001.

6 S.-H. Guo, S.-J. Tsai, H.-C. Kan, D.-H. Tsai, M. R. Zachariah and R. J. Phaneuf, *Adv. Mater.*, 2008, **20**, 1424–1428.

7 S. W. Hell and J. Wichmann, *Opt. Lett.*, 1994, **19**, 780–782.

8 S. W. Hell and M. Kroug, *Appl. Phys. B Lasers Opt.*, 1995, **60**, 495–497.

9 E. Betzig, *Opt. Lett.*, 1995, **20**, 237–239.

10 E. Betzig, G. H. Patterson, R. Sougrat, O. W. Lindwasser, S. Olenych, J. S. Bonifacino, M. W. Davidson, J. Lippincott-Schwartz and H. F. Hess, *Science*, 2006, **313**, 1642–1645.

11 R. M. Dickson, A. B. Cubitt, R. Y. Tsien and W. E. Moerner, *Nature*, 1997, **388**, 355–358.

12 J. Enderlein, T. Ruckstuhl and S. Seeger, *Appl. Opt.*, 1999, **38**, 724–732.

13 T. Ruckstuhl, J. Enderlein, S. Jung and S. Seeger, *Anal. Chem.*, 2000, **72**, 2117–2123.

14 T. Ruckstuhl, M. Rankl and S. Seeger, *Biosens. Bioelectron.*, 2003, **18**, 1193–1199.

15 T. Ruckstuhl, C. Winterflood and S. Seeger, *Anal. Chem.*, 2011, **83**, 2345–2350.

16 T. Ruckstuhl and D. Verdes, *Opt. Express*, 2004, **12**, 2783–2784.

17 T. Barroca, K. Balaa, J. Delahaye, S. Lévêque-Fort and E. Fort, *Opt. Lett.*, 2011, **36**, 3051–3.

18 T. Barroca, K. Balaa, S. Lévêque-Fort and E. Fort, *Phys. Rev. Lett.*, 2012, **108**, 218101.

19 D. Kurzbuch, M. Somers and C. McDonagh, *Opt. Express*, 2013, **21**, 22070–5.

20 C. M. Winterflood, T. Ruckstuhl, D. Verdes and S. Seeger, *Phys. Rev. Lett.*, 2010, **105**, 108103.

21 D. Hill, B. McDonnell, S. Hearty, L. Basabe-Desmonts, R. Blue, M. Trnavsky, C. McAtamney, R. O'Kennedy and B. D. MacCraith, *Biomed. Microdevices*, 2011, **13**, 759–767.

22 X. Li, Y. Ding, J. Shao, H. Tian and H. Liu, *Adv. Mater.*, 2012, **24**, OP165–OP169.

23 Y. Sun, I. Perch-Nielsen, Z. Wang, D. Bang and A. Wolff, in *Micro Total Analysis Systems 2012*, 2012, pp. 1315–1317.

24 Y. Sun, I. Perch-Nielsen, M. Dufva, D. Sabourin, D. D. Bang, J. Høgberg and A. Wolff, *Anal. Bioanal. Chem.*, 2012, **402**, 741–8.

25 E. Berthier, E. W. K. Young and D. Beebe, *Lab Chip*, 2012, **12**, 1224–37.

26 C. A. Schneider, W. S. Rasband and K. W. Eliceiri, *Nat. Methods*, 2012, **9**, 671–675.